INT. COMM. HEAT MASS TRANSFER
Vol. 19, pp. 721-731, 1992
Printed in the USA

0735-1933/92 $5.00 + .00
Copyright©1992 Pergamon Press Ltd.

A NOTE ON HIGH SCHMIDT NUMBER LAMINAR BUOYANT JETS DISCHARGED HORIZONTALLY

Anupam Dewan, Jaywant H.Arakeri and J.Srinivasan
Department of Mechanical Engineering
Indian Institute of Science, Bangalore-560 012, INDIA.

(Communicated by D.B. Spalding and B.R. Pai)

ABSTRACT

A new model has been developed for the integral analysis of high Schmidt number (or equivalently high Prandtl number) laminar buoyant jets discharged horizontally. This model assumes top-hat density profile across the inner core of jet and Gaussian velocity profile. Entrainment coefficient corresponding to pure laminar jet has been taken in the analysis. The prediction of the jet trajectory agree well with experimental data in the regions where the jet remains laminar.

Introduction

Buoyant jets are important in a variety of fields such as oceanography, meteorology and environmental studies and in some engineering applications like solar ponds. In solar ponds, negatively buoyant jets occur during the repair of gradient zone. The gradient zone in the solar pond can break down due to local instabilities. To reconstruct the density profile, saline water from the bottom of pond is injected horizontally into the gradient zone by means of a diffuser. Density of this injected fluid is higher than that of surrounding fluid and thus the jet is negatively buoyant. The effectiveness of this jet in reconstruction of the gradient zone is dependent upon maintaining an almost horizontal trajectory and minimum spread of the jet. To maintain a horizontal jet trajectory, the initial momentum should be high compared to buoyancy. In other words, the discharge Froude number Fr should be high. It may be noted that Fr^{-2} is equal to Gr/Re^2, the mixed convection parameter, where Gr is the Grashof number and Re is discharge Reynolds number. To minimize the spread of the jet,

the jet should be laminar and therefore, the discharge Reynolds number Re should be low. In the present work, the trajectory of a laminar buoyant jet has been studied as a function of discharge Froude number and discharge Reynolds number. Since we are concerned with the situations occuring in solar ponds, we consider the case where Schmidt number Sc is equal to 745. This is the value encountered when a saline jet is discharged.

Since most of the buoyant jet flows arising in practice are turbulent, a lot of work has been done on turbulent buoyant jets. Laminar buoyant jets are of interest in solar ponds and also in laboratory studies. Abraham [1] has analysed the behaviour of a turbulent jet discharged horizontally into a homogeneous denser ambient. His solution follows the integral approach with the assumption of similar Gaussian velocity and buoyancy profiles across the jet. Brand and Lahey [2] solved boundary-layer equations for the steady laminar flow of a vertical jet, including a buoyancy term caused by temperature difference. Mollendorf and Gebhart [3] performed a perturbation analysis which included the effect of small amount of thermal buoyancy on velocity and temperature fields of a round, laminar and vertical jet. Tenner and Gebhart [4] conducted experiments on steady state flow of fresh and salt water, vertical, axisymmetric, laminar buoyant jets in a stably-stratified salt water environment. They concluded that such a jet induces the flow of a toroidal jet around itself. Satyanarayana and Jaluria [5] carried out an experimental study of round, laminar, hot water buoyant jets discharged at an inclination to the vertical buoyancy force. They studied the trajectory and thermal characteristics of the jet as a function of mixed convection parameter Gr/Re^2. They also used integral analysis with same Gaussian profiles for both velocity and density difference. In their analysis, they used a constant value of entrainment coefficient α equal to 0.07. This value of α corresponds to turbulent buoyant jets and plumes flows. The Reynolds number used by them is in the range of 530 - 1376 and therfore, it is possible that the buoyant jets they studied were not laminar. They were mainly concerned with regions very close to jet exit. Hence, their analysis is not useful for solar pond application.

Problem Formulation and Method of Analysis

We consider the problem of a laminar buoyant jet discharged horizontally into an ambient of uniform density. The whole system i.e., the jet and the surroundings is assumed to be at the same temperature. Thus buoyancy is assumed to arise only due to concentration difference between the jet fluid and the ambient fluid. Governing equations used in the analysis are the integral form of the laws of conservation of mass, horizontal and vertical momenta, and the species. The problem was solved using integral method because this is adequate for predicting the jet trajectory. Following assumptions are used in the analysis : (i) The fluid is incompressible, (ii) Boussinesq approximation is valid i.e., the density difference is considered only in buoyancy term, (iii) Flow field is axisymmetric about the centerline of

jet, (iv) Velocity and density profiles are similar at all locations along the jet centerline and (v) Rate of entrainment of surrounding fluid into the jet flow is proportional to jet centerline velocity and a characteristic jet width.

The governing equations in cylindrical co-ordinate system are as follows (where s is the distance along jet centerline, r is the radial distance from jet centerline, θ is local jet centerline angle with horizontal and u is local velocity component along jet centerline):

$$\text{Continuity}: \quad \frac{d}{ds}\int_0^\infty u\, 2\pi r dr = \alpha\, 2\pi b u_c \tag{1}$$

$$\text{Conservation of horizontal momentum}: \quad \frac{d}{ds}\int_0^\infty u^2\, 2\pi r dr\, \cos\theta = 0 \tag{2}$$

$$\text{Conservation of vertical momentum}: \quad \frac{d}{ds}\int_0^\infty u^2\, 2\pi r dr\, \sin\theta = \int_0^\infty g\,\frac{\Delta\rho}{\rho}\, 2\pi r dr \tag{3}$$

$$\text{Conservation of species}: \quad \frac{d}{ds}\int_0^{r_s} \Delta\rho\, u\, 2\pi r dr = 0 \tag{4}$$

where α, the proportionality constant, is known as entrainment coefficient and r_s is the radius of core. The (x, y) co-ordinates of jet centerline are given by :

$$dx = ds\,\cos\theta \qquad dy = ds\,\sin\theta$$

Velocity and density profiles assumed are :

$$\begin{aligned} u &= u_c\, e^{-r^2/b^2} \\ \Delta\rho &= \rho_i - \rho_a = \text{constant} \quad \text{for } r \le r_s \\ \Delta\rho &= \rho_i - \rho_a = 0.0 \quad \text{for } r > r_s \end{aligned}$$

where b is the radial location at which velocity u is $1/e$ times the centerline velocity u_c (e is the exponential). It may be noted here that this assumption would be appropriate for a laminar jet when the Schmidt number Sc tends to infinity i.e., diffusivity of species D_m is negligible compared to momentum diffusivity ν.

These profiles were substituted in the governing equations and integration was carried out. The resulting equations were separated to get individual equations for centerline velocity u_c, jet width b, local jet centerline angle θ and radius of core r_s. These equations were non-dimensionalized using variables given below:

$$\begin{aligned} \text{Length} \quad & X = x/D \quad Y = y/D \quad S = s/D \\ & B = b/D \quad R_s = r_s/D \\ \text{Velocity} \quad & U = u/u_i \quad U_c = u_c/u_i \end{aligned}$$

$$\text{Density difference} \quad \phi = (\rho - \rho_a)/(\rho_i - \rho_a) \qquad \phi_c = (\rho_c - \rho_a)/(\rho_i - \rho_a)$$

where D is the internal diameter of discharge tube, u_i is average discharge velocity and subscripts c and a denote centerline and ambient conditions respectively. ϕ_c is a constant, equal to 1.0 as $\rho_c = \rho_i$. The non-dimensionalized equations are:

$$\frac{dU_c}{dS} = \frac{2}{Fr^2}\frac{\phi_c}{U_c}\frac{Rs^2}{B^2}\sin\theta - \frac{2\alpha U_c}{B} \tag{5}$$

$$\frac{dB}{dS} = 2\alpha - \frac{1}{Fr^2}\frac{\phi_c}{U_c^2}\frac{Rs^2}{B^2}B\sin\theta \tag{6}$$

$$\frac{d\theta}{dS} = \frac{2}{Fr^2}\frac{\phi_c}{U_c^2}\frac{Rs^2}{B^2}\cos\theta \tag{7}$$

$$R_s = B\sqrt{\log_e\left\{\frac{1}{1 - \frac{constant}{U_c\phi_c B^2}}\right\}} \tag{8}$$

where $Fr = \dfrac{u_j}{\sqrt{gD\dfrac{\Delta\rho_o}{\rho_o}}}$ is the discharge Froude number, $dX = dS\cos\theta$ and $dY = dS\sin\theta$. Subscript o denotes discharge conditions.

These coupled first order ordinary differential equations were solved numerically (with S as the independent variable) as an initial value problem for various values of discharge Froude number Fr and discharge Reynolds number Re. Entrainment coefficient α corresponding to pure laminar jet was determined from Schlichting's [6] exact solution. According to this, volume flow rate Q at any location $= 8\pi\nu s$ therefore, $\frac{dQ}{dS} = 8\pi\nu = \alpha\, 2\pi b u_c$ or, $\alpha = \frac{4.9}{Re}$ where $Re = \frac{u_i D}{\nu}$. It may be noted that product bu_c has a constant value for a pure laminar jet.

The solutions of these non-dimensionalised equations yield jet centerline velocity U_c, jet width B, local jet angle θ, width of the core R_s and (X, Y) co-ordinates of jet centerline. Hamming's multistep predictor-corrector method was used for numerical solutions. For this method, the three starting values from the initial conditions were generated using fourth-order Runge-Kutta method. The advantage of using multi step methods is that these methods generally require less computational effort per step than the single step Runge-Kutta methods for comparable accuracy. To determine initial conditions, following assumptions were made : (i) Velocity and density profiles in the flow under consideration develop from fully developed laminar pipe flow leading to horizontal discharge of buoyant jet, (ii) Mass, momentum and species are conserved during this development, (iii) The jet remains horizontal and (iv) Jet origin is located at discharge point ($S = 0$). Six initial conditions determined from these assumptions are (for details see Dewan [8]):

$$\begin{array}{llllll} U_c = 2.297 & B = 0.355 & R_s = 0.5 \\ X = 0.0 & Y = 0.0 & \theta = 0.0 \end{array}$$

$R_s = 0.5$ means that initially radius of core is equal to internal radius of discharge tube. Constant in equation (8) can be determined from initial conditions and is equal to 0.25.

However, if Gaussian density profile $\Delta\rho = \Delta\rho_c\, e^{-r^2/b^2}$ along with Gaussian velocity profile $u = u_c\, e^{-r^2/b^2}$ is taken in the analysis, then the resulting equations in dimensionless form as well as initial conditions are different. The difference is that the term R_s/B is equal to 1 in equations (5,6,7) and equation (8) coming from the equation for conservation of species, which is integrated from 0 to ∞, is as follows:

$$U_c \phi_c B^2 = constant \tag{9}$$

Initial conditions in this case are:

$$U_c = \frac{8\rho_i}{4\rho_i - \rho_a} \qquad B = \sqrt{\frac{4\rho_i - \rho_a}{32\rho_i}} \qquad \phi_c = 2.0$$
$$X = 0.0 \qquad Y = 0.0 \qquad \theta = 0.0$$

Experimental Set-up and Methodology

Figure 1 is the schematic representation of experimental set-up. Pure water was discharged horizontally into a salt water solution of uniform density contained in a glass tank of inside dimensions $0.30 \times 0.36 \times 0.60$ m. Shadowgraph technique was used to trace the trajectory of the jet. Maximum expected error involved in tracing the trajectory was less than 1 mm. Flow rate was controlled by means of a capillary fine control valve 5. A tube of internal diameter 1.0 mm was used as jet. To measure flow rate, following procedure was adopted:

1. Measure flow rate from the beaker using a 10 ml burette.
2. Introduce flexible PVC tubing into the capillary joined to the top of aspirator bottle without disturbing the valve 5 controlling flow from the beaker.
3. Adjust valve 5 controlling the flow to discharge tube in such a way that the water level in the capillary remains constant. This results in a constant discharge rate, equal in value to flow rate measured in 1.

The beaker functioned as a constant head source. Density of salt solution was determined using calibrated hydrometers. A 3.0 mm capillary was used to ensure that the jet flow rate and the flow rate from the beaker were accurately matched. Therefore, any mismatch between two flow rates could be easily observed. Maximum expected uncertainties in calculations of discharge Froude number Fr and discharge Reynolds number Re were 12% and 9% respectively. These were mainly because of error involved in flow rate measurement.

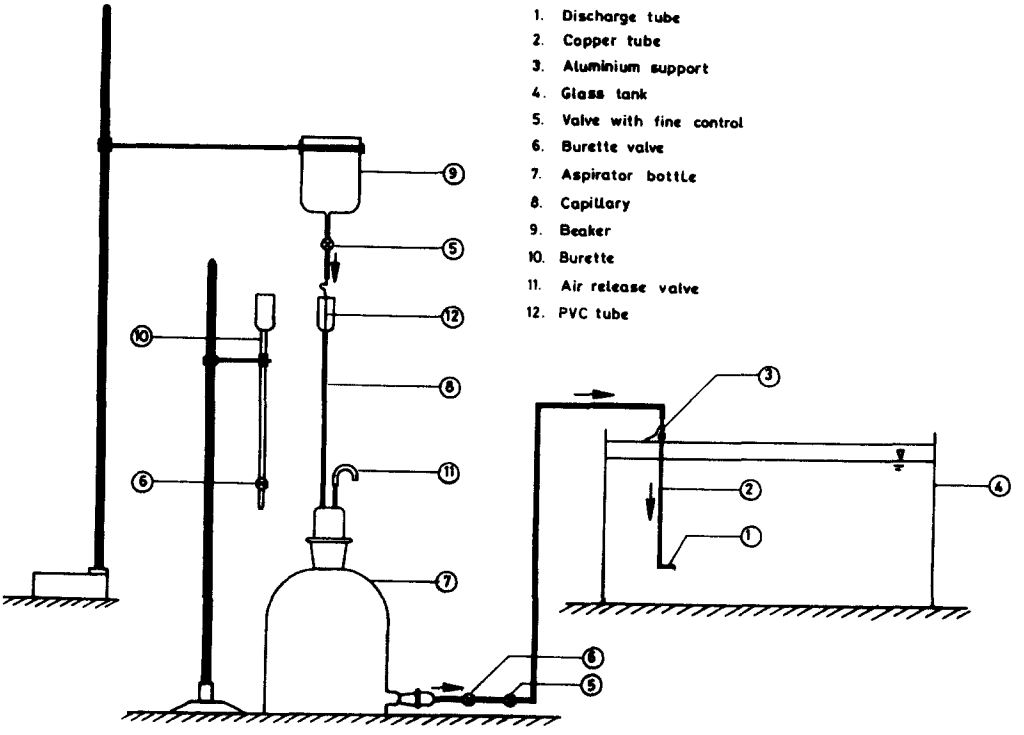


FIG.1
Schematic representation of experimental set-up.

Results and Discussion

The difference in the jet trajectory predicted by the two models is shown in figure 2. In figure 2a, the jet trajectory obtained by assuming Gaussian velocity and density profiles is shown for $Fr = 22.4$ and $Re = 220.2$. In figure 2b, the predictions of the model with Gaussain velocity and top hat density profiles is shown for same Fr and Re as in figure 2a. We find that the predictions of the model using top hat density profile agrees better with observations than the model with Gaussain density profile. The model with Gaussian density profile tends to predict a jet trajectory which was always higher than the observed jet trajectory. This is because the jet with Gaussian density profile is more buoyant than a jet with top hat density profile, as the buoyancy gets distributed over larger area compared to the model with top hat density profile. It means that this Gaussian density profile is

inappropriate for the case of high Schmidt number laminar buoyant jets, as it corresponds to a case of Sc equal to one, where both velocity and density profiles spread by equal amount.

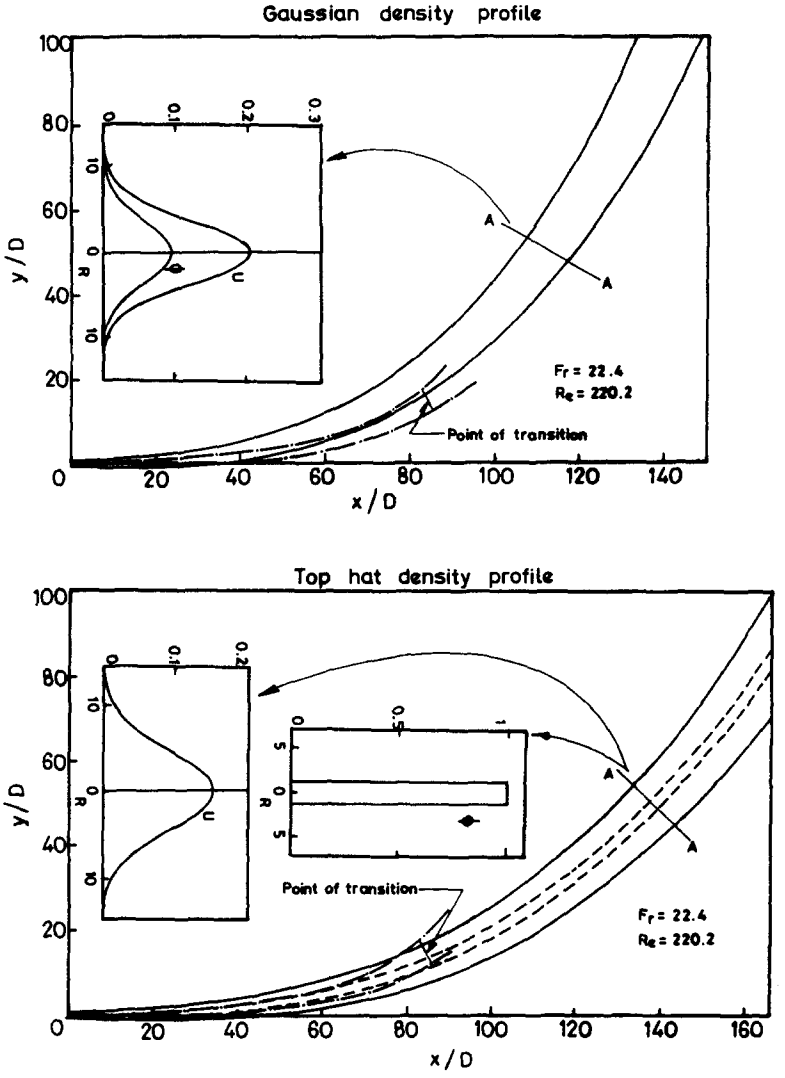


FIG.2
Comparison between prediction and experimental observation of jet trajectory.
(a) —— prediction of the model with Gaussian density profile, — — —experiment.
(b)- - - - prediction of the model with top-hat density profile, — — —experiment.

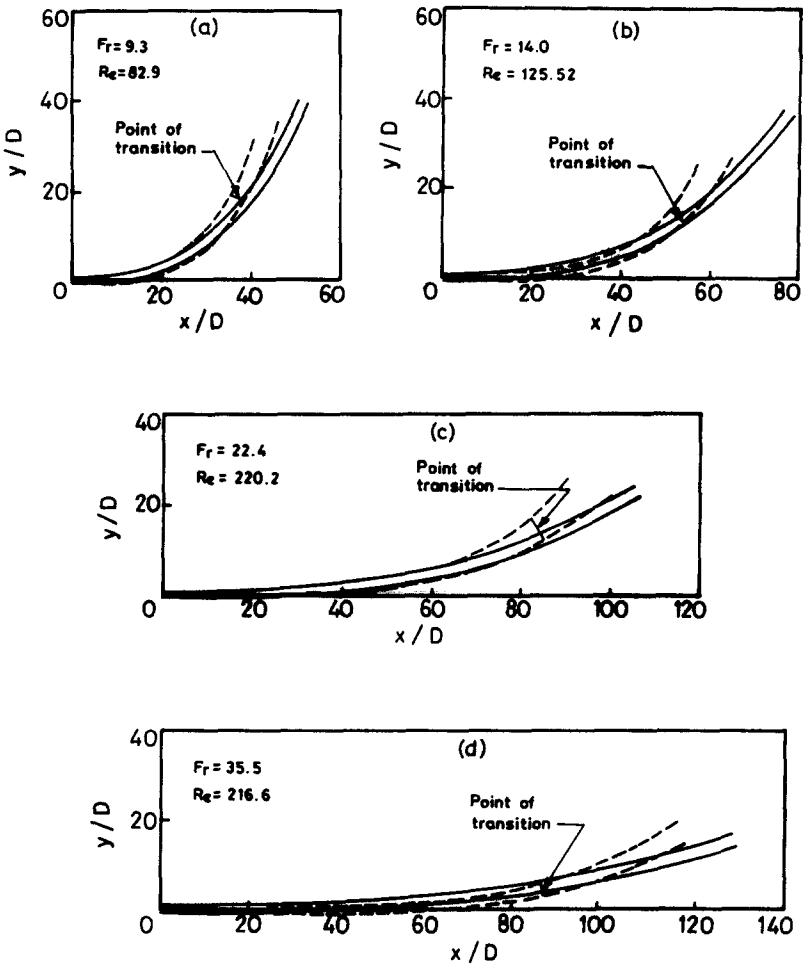


FIG.3
Comparison between predictions of the model with top-hat density profile and experimental observations of jet trajectory. —— predictions,——— experiments.

The comparison between predictions of the model with top hat density profile and experimental observations is shown in figure 3 for various values of Fr and Re. We find that in all cases the agreement between predictions and observations is good upto the point of transition. In the experimental observations, the transition of the laminar jet to a turbulent jet could be observed easily in the shadowgraph on account of the sudden increase in the width of the jet. In figure 3c, we find that deviation between predictions and observations occurs even before the onset of transition. This could be on account of our assumption of

entrainment coefficient based on pure laminar jet. As the jet begins to curve upwards, the buoyancy effects become dominant and hence the value of entrainment coefficient based on pure laminar jet will be inappropriate. For the range of Re we have considered the use of entrainment coefficient based on pure laminar jet seems to be adequate to predict the jet trajectory before transition.

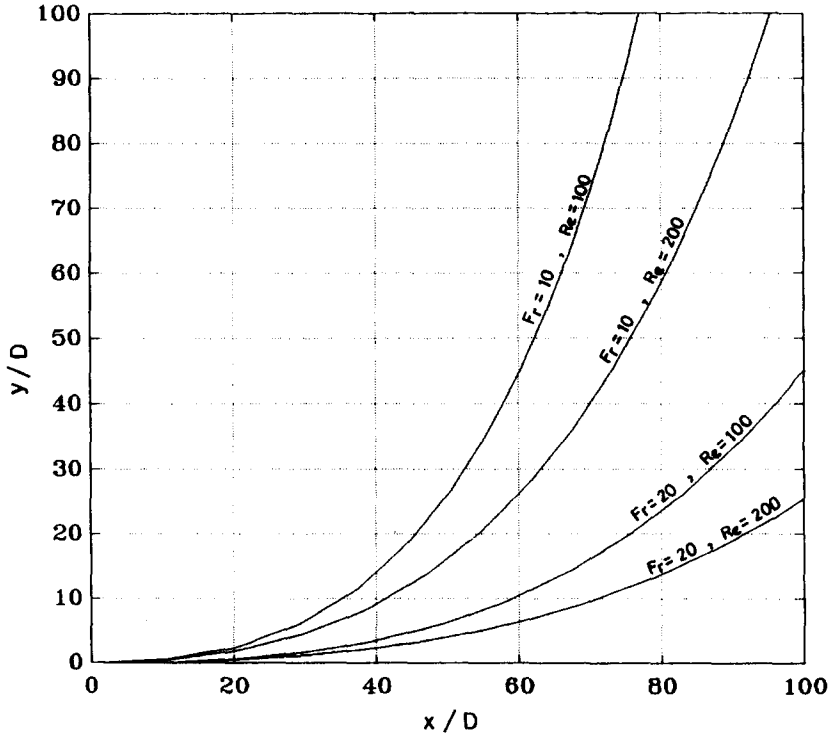


FIG.4
Effect of variation in Fr and Re on predicted centerline jet trajectory.

The effect of variation in Fr and Re on predicted centerline jet trajectory is shown in figure 4. We find that the doubling of Fr has a greater impact on the jet trajectory than the doubling of Re. When Re is decreased, the α increases and hence it leads to jet becoming more buoyant. A higher value of α means more quiescent ambient fluid is entrained, thereby increasing its volume with consequent reduction in velocity as horizontal momentum is always conserved. As a result of this, horizontal velocity reduces more rapidly as compared to the case of lower α. Initially any horizontally discharged buoyant jet is driven mainly by momentum imparted to it, therefore, an increase in α means jet traversing lesser horizontal

distance i.e., it will appear to be more buoyant. If the velocity of the jet is doubled, both Re and Fr are doubled and this changes the jet trajectory dramatically. Therefore, it is clear that Reynolds number dependance of such jets has to be taken into account to determine correct entrainment coefficient α, whereas, for turbulent jets α is independent of Reynolds number and is equal to 0.057.

From the figures 2 and 3 we also observe that initially at the discharge point, diameter of the core $2R_s$ is equal to internal diameter of discharge tube D and subsequently downstream it increases. This increase in R_s is due to the entrainment of quiescent ambient fluid into the jet fluid. Owing to this entrainment, velocity of the jet gets reduced because horizontal momentum is always conserved. As diffusivity of mass D_m is very small compared to momentum diffusivity ν i.e., high value of Schmidt number Sc, species are conserved inside the core, and hence the reduction in velocity causes the radius of the core to increase. It may also be noted that as the jet trajectory becomes more vertical, we need to modify the entrainment coefficient for plume-like behaviour. In the case of laminar plumes, Yih [8] has shown that the velocity profile is not Gaussian. Hence one has to incorporate the change in entrainment coefficient and velocity profile to predict the trajectory of buoyant jets .

Conclusions

We have shown that the model with Gaussian density profile is not appropriate for the case of high Schmidt number laminar buoyant jets. This results in the prediction of a more buoyant jet than that observed. A model with top hat density profile is more appropriate in such cases. The entrainment coefficient based on pure laminar jet is found to be adequate if jet is not highly buoyant ($Fr > 10$, $Re > 100$).

Nomenclature

b	jet width based on Gaussian velocity profile $u = u_c\, e^{-r^2/b^2}$
B	non-dimensional jet width
D	internal diameter of discharge tube
D_m	diffusivity of species
Fr	densimetric Froude number $= \dfrac{u_i}{\sqrt{gD\dfrac{\Delta\rho_o}{\rho_o}}}$
g	acceleration due to gravity
r	radial distance from jet centerline
r_s	radius of jet's core

R	non-dimensional radial distance from jet centerline
Re	discharge Reynolds number $= \frac{u_i D}{\nu}$
s	distance along jet centerline
S	non-dimensional distance along jet centerline
Sc	Schmidt number $= \frac{\nu}{D_m}$
u	local velocity component along jet centerline
u_c	local centerline jet velocity
u_i	average discharge velocity
U	non-dimensional local jet velocity
U_c	non-dimensional local jet centerline velocity
x, y	co-ordinates of jet centerline
X, Y	non-dimensional co-ordinates of jet centerline

Greek Symbols

α	entrainment coefficient
ν	kinematic viscosity
ρ	fluid density
θ	angle of inclination of jet centerline with the horizontal
ϕ	non-dimensional density difference
ϕ_c	non-dimensional centerline density difference

References

1. G.Abraham, ASCE J. Hydraulic Division, *91*, 139 (1965).
2. R.S.Brand and F.J.Lahey, J. Fluid Mech., *29*, 305 (1967).
3. J.C.Mollendorf and B.Gebhart, Int. J. Heat Mass Transfer, *16*, 735 (1973).
4. A.R.Tenner and B.Gebhart, Int. J. Heat Mass Transfer, *14*, 2051, (1971).
5. S.Satyanarayana and Y.Jaluria, Int. J. Heat Mass Transfer, *25*, 1569 (1982).
6. H.Schlichting, *Boundary Layer Theory*, p.181. McGraw-Hill Book Company, New York (1968).
7. Anupam Dewan, M.E. Dissertation, Dept. of Mech. Engg., Indian Institute of Science, Bangalore, India (Jan. 1991).
8. C.-S.Yih, Proc. Ist U.S. Nat. Cong. Appl. Mech., 941 (1951).

Received May 4, 1992